

## REPORT DOCUMENTATION PAGE

AD-A255 505

Public reporting burden for this collection of information is estimated to average 1 hour per response, including gathering and maintaining the data needed, and completing and reviewing the collection of information collection of information, including suggestions for reducing this burden, to Washington Headquarters Services, Directorate for Information Operations and Reports, 1215 Jefferson Davis Highway, Suite 1204, Arlington, VA 22202-4302, and to the Office of Management and Budget, Paperwork Project, Washington, DC 20503.



Source  
of this  
document

1. AGENCY USE ONLY (Leave blank)		2. REPORT DATE July 31, 1992		3. REPORT TYPE AND DATES COVERED Final 1 March 1991 - 31 May 1992	
4. TITLE AND SUBTITLE Intrinsic Bistable Photonic Materials by Copper Colloid Formation in Silica				5. FUNDING NUMBERS  ② DAALO3-91-G-0028	
6. AUTHOR(S) Robert H. Magruder, III				7. PERFORMING ORGANIZATION NAME(S) AND ADDRESS(ES) Vanderbilt University Nashville, TN 37240	
8. PERFORMING ORGANIZATION REPORT NUMBER				9. SPONSORING / MONITORING AGENCY NAME(S) AND ADDRESS(ES) U. S. Army Research Office P. O. Box 12211 Research Triangle Park, NC 27709-2211	
10. SPONSORING / MONITORING AGENCY REPORT NUMBER ARO 28109.8-MS				11. SUPPLEMENTARY NOTES The view, opinions and/or findings contained in this report are those of the author(s) and should not be construed as an official Department of the Army position, policy, or decision, unless so designated by other documentation.	
12a. DISTRIBUTION / AVAILABILITY STATEMENT Approved for public release; distribution unlimited.				12b. DISTRIBUTION CODE	
13. ABSTRACT (Maximum 200 words) Ion implantation has been used to assemble planar thin films of metallic nanoclusters embedded in a dielectric. Gold and copper were both found to produce nanosize metal clusters in silica. Both the size and size distribution of the metallic nanoclusters were characterized by transmission electron microscopy. The size and size distribution were found to be controlled by implantation protocols and post implantation processing. The linear and nonlinear optical properties were measured and found to be a function of the cluster size and size distribution. The nonlinear response was electronic in character and has a response time which is no longer than 15 ps. The nonlinear index of refraction of these materials has a magnitude $\sim 10^{-10} \text{ cm}^2 \text{ W}^{-1}$ , comparing favorably to semi-conductor microcrystallites. The linear optical properties were well described by Mie theory while the nonlinear responses can be described by effective medium theory.					
14. SUBJECT TERMS metal colloids, optical properties of metallic colloids				15. NUMBER OF PAGES 16	
16. PRICE CODE				17. SECURITY CLASSIFICATION OF REPORT UNCLASSIFIED	
18. SECURITY CLASSIFICATION UNCLASSIFIED		19. SECURITY CLASSIFICATION OF ABSTRACT UNCLASSIFIED		20. LIMITATION OF ABSTRACT UL	

92 9 02 083

**Final Report to the Army Research Office**

**Contract # DAAL03-91G-0028**

**Intrinsic Bistable Photonic Materials  
By Copper Colloid Formation in Silica**

**Robert H. Magruder, III  
Principal Investigator**

**July 31, 1992**

Accession For	
NTIS CRA&I	<input checked="" type="checkbox"/>
DTIC TAB	<input type="checkbox"/>
Unannounced	<input type="checkbox"/>
Justification	
By	
Distribution /	
Availability Codes	
Dist	Avail and/or Special
A-1	

**92-24357**



1788.

## Table of Contents

Objectives, Motivation and Accomplishments .....	1
Summary of Experimental Program .....	1
Sample Preparation and Physical Characterization .....	2
Linear Optical Characterization .....	5
Nonlinear Optical Characterization .....	7
Summary of Results for Au Implanted $\text{Al}_2\text{O}_3$ .....	10
Implications for Bistable Device Development .....	10
Personnel .....	11
References .....	11
Publications .....	13

## Objectives, Motivation and Accomplishments

This one-year feasibility study was focused on preparation, characterization and control of intrinsic bistable photonic materials in a unique form: a bistable cluster composite, in a planar waveguide geometry, consisting of nanosize metallic clusters in high-purity silica. Our goals in the research were (1) to demonstrate the ability to control the size and size distribution of the metallic clusters; (2) to ascertain the effects of the materials processing techniques on the optical properties of the nanocluster composite; and (3) to investigate the magnitude, response time and mechanism of the nonlinear optical response. In our experiments, a metal nanocluster composite was formed by ion implantation, followed in some cases by annealing.

Ion implantation offers important advantages in the formation of optically bistable composite materials: First, the depth and width of the thin layers can be controlled by changing the ion implantation energy. Second, nonequilibrium concentrations and phases of the composites can be assembled. Third, ion implantation is a processing technique compatible with microelectronics fabrication, offering the potential for ready integration into hybrid opto-electronic devices.

In the course of the year-long funding period, we were able to achieve all of the stated goals of the original proposal, successfully demonstrating that:

- substrate temperature, total ion dose and ion dose rate affect both size distributions and optical properties of the nanocomposite materials;
- that the linear optical properties can be described by Mie theory while the nonlinear responses are reasonably described by effective medium theory;
- the nonlinear index of refraction of these materials has a magnitude  $\sim 10^{-10} \text{ cm}^2 \text{ W}^{-1}$ , comparing favorably to that of semi-conductor microcrystallites, such as CdS;
- the optical nonlinearity in these nanocomposite materials is electronic in character, and has a response time which is no slower than 15 ps.

In addition, we have developed a new theoretical treatment for nonlinear index measurements in thin films, and made some observations which suggest a new technique for measuring the quantum confinement effect in Au-implanted silica. Our results suggest that it may be possible to create fast bistable switching devices by implanting metal ions in insulators whose nonlinear response can be controlled by choice of implanted metal ion and by processing conditions.

## Summary of Experimental Program

Control of substrate temperature during implantation, dose rate and post implantation processing were used to alter the size and size distribution of the colloids formed. The size distributions were characterized by TEM, the linear optical properties by absorption measurements and the nonlinear optical measurements by forward degenerate four wave mixing and the z-scan technique.

Metallic colloid formation was achieved in both Cu implanted and Au implanted glasses. The wavelength of the surface plasmon resonance due to the colloids was dependent upon ion type. These glass composite materials exhibited third order nonlinear susceptibilities on the order of  $10^{-9}$  esu, some four orders of magnitude larger than that of pure fused silica. The wavelength of the maximum nonlinear response was dependent upon ion type.

## Sample Preparation and Physical Characterization

Cu and Au ions were implanted in Spectrosil A and Corning 7940 substrates; a limited number of preparations were made in single crystal  $\text{Al}_2\text{O}_3$ . The Cu ions were typically implanted at 160 keV at various doses, substrate temperatures and dose rates. The implantation protocols are given in Table 1.

Table 1  
Implantation Parameters for Cu Implanted Silica

Nominal Dose ( $\times 10^{16}$ )	Substrate Temperature (°K)	Dose Rate $\mu\text{A}/\text{cm}^2$
12	295	2.5
6	295	0.7
6	295	2.5
6	295	5.0
6	295	7.5
6	100	2.5
6	295	2.5
6	693	2.5
3	295	2.5
3	100	2.5
3	693	2.5
3	295	7.5
1	295	2.5
1	295	7.5
0.5	295	2.5
0.3	295	2.5

Corning 7940 substrates were used for all the Au implantations in silica. The Au ions were implanted at 2.75 MeV with doses of 6 and  $12 \times 10^{16}$  ions/cm<sup>2</sup>. Samples were subsequently annealed in Ar + 4% H<sub>2</sub> and in O<sub>2</sub>. Single crystal  $\text{Al}_2\text{O}_3$  substrates were also implanted with Au ions with doses ranging from 1.1 to  $12 \times 10^{16}$  ions/cm<sup>2</sup>.

All samples were analyzed by Rutherford backscattering to determine ion depth profiles. For doses  $\geq 3 \times 10^{16}$  ions/cm<sup>2</sup> the distributions were found to be bimodal while for doses  $< 3 \times 10^{16}$  ions/cm<sup>2</sup> the distributions were found to be Gaussian. The Au implanted samples show only the Gaussian distribution for all doses. Subsequent thermal annealing of the Au implanted glasses did not affect the ion depth or profile.

Standard bright field (BF)/ dark field (DF) imaging and electron diffraction techniques were used to characterize the implanted layer for the Cu implanted silica. All the samples exhibit spherical particles embedded in the silica matrix. Tilting the sample  $\pm 45^\circ$  revealed that these clusters are spherical in shape with random crystallographic orientation. Electron diffraction patterns display the ring pattern characteristic of face centered cubic (FCC) polycrystalline metallic copper, superimposed on the diffuse diffracted intensity from the amorphous silica matrix. Figure 1 shows a DF micrograph and ring pattern for a sample implanted with  $12 \times 10^{16}$  ions/cm<sup>2</sup>.

Nanocluster size and size distributions in the Cu implanted silica were measured by transmission electron microscopy. The volume fraction of colloids that were detectable by TEM, particle size and the standard deviation of particle size were dependent on total dose, dose rate and substrate temperature during implantation. The smallest particles observed are  $\sim 2$  nm in size which corresponds to approximately 350 Cu atoms. It is not clear if 2 nm represents the smallest particle or a resolution limit from the diffraction and phase contrast mechanisms.

Figure 1. Dark field image of metallic Cu nanoclusters in sample implanted with  $12 \times 10^{16}$  ions/cm<sup>2</sup>. Insert: Electron diffraction image of the ring pattern characteristic of face centered cubic copper.

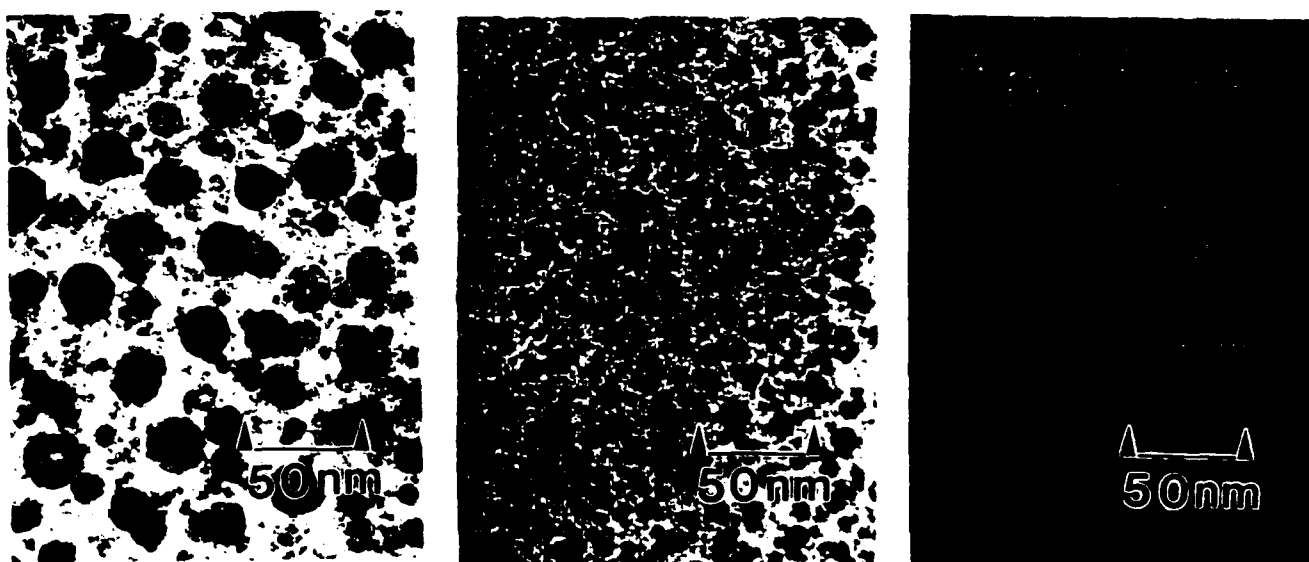


Figure 2. Bright field TEM images of Cu nanoclusters for samples implanted with  $12 \times 10^{16}$ ,  $6 \times 10^{16}$  and  $3 \times 10^{16}$  ions/cm<sup>2</sup> (left to right).

Figure 2 shows the micrographs for samples implanted with doses of 3, 6, and  $12 \times 10^{16}$  ions/cm<sup>2</sup> at a substrate temperature of 295 K and a dose rate of  $2.5 \mu\text{amps/cm}^2$ . The mean particle size and size distribution increase with increasing total dose. The statistical distributions of sizes for the Cu nanoclusters for the 3 and  $12 \times 10^{16}$  ions/cm<sup>2</sup> samples are shown in figure 3.

Increasing the substrate temperature during implantation produced particles with a larger mean size but a smaller variance in size than found either by varying the total dose or dose rate. The results are summarized in Table 2 which lists the mean particle size, the standard deviation, dose as measured by RBS, dose as calculated from the TEM measurements and the volume fraction of Cu for a series of Cu implanted glasses.

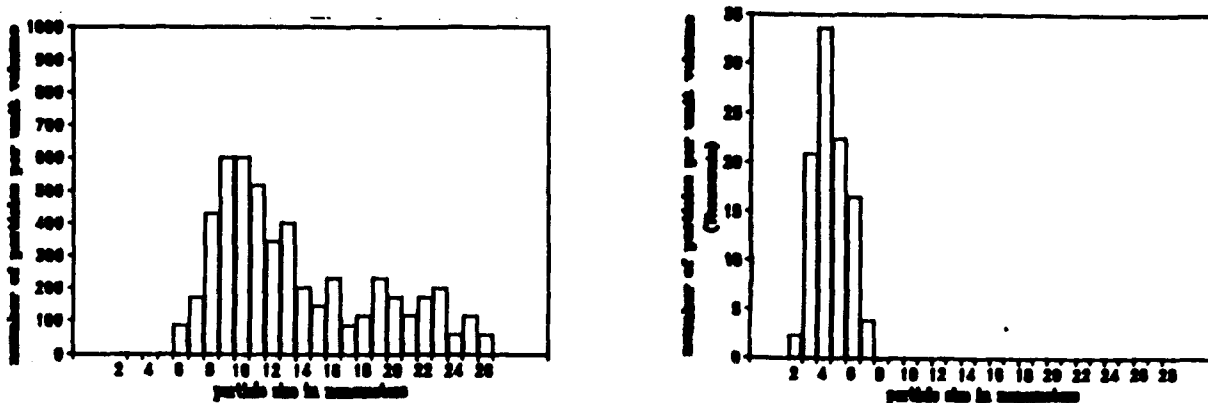


Figure 3. Statistical distributions of sizes for Cu nanoclusters (left) for sample implanted with  $12 \times 10^{16}$  ions/cm<sup>2</sup> and (right) for sample implanted with  $3 \times 10^{16}$  ions/cm<sup>2</sup>.

Table 2

Particle size measured for various dose and implantation temperatures at dose rate of  $2.5 \mu\text{A}/\text{cm}^2$

Nominal Implant Dose ( $10^{16}\text{cm}^{-2}$ )	Mean Particle Size Size(nm)	Standard Deviation (nm)	Volume Fraction (%)	Computed Density ( $10^{16}$ )	RBS ( $\times 10^{16}$ )	Temperature (K)
12	10.1	5.4	7.5	9.5	10	295
6	7.0	2.1	1.6	2.1	5.3	295
3	4.3	1.1	0.5	0.7	2.8	295
6	11.8	3.8	3.5	4.5	5.2	673
6	7.0	2.1	1.6	2.1	5.4	295
6	7.2	2.5	1.7	2.3	5.4	100

Table 3

Dose rate dependence for samples implanted with Cu to a nominal dose of  $6 \times 10^{16}$  ions/cm<sup>2</sup>

Dose Rate ( $\mu\text{A}/\text{cm}^2$ )	Mean Particle Size (nm)	Standard Deviation (nm)	Volume Fraction	Computed Dose ( $10^{16}$ )	RBS ( $10^{16}$ )
7.5	$12.6 \pm 3$	$5.7 \pm 2$	3.8	4.8	5.1
5.0	9.9	4.3	2.3	2.8	5.2
2.5	6.7	1.9	1.4	1.8	5.3
0.7	5.2	1.5	0.7	0.9	5.6

The dose rate also affects the mean particle size as seen from Table 3. Increasing the dose rate from  $0.7$  to  $7.5 \mu\text{A}/\text{cm}^2$  increases mean particle size from  $5.2$  to  $12.6$  nm. However, varying the substrate temperature yields a large mean particle size with a smaller variance than variations in either dose or dose rate, suggesting that substrate temperature may be the most effective method of controlling particle size. From Table 3 it is clear that not all the Cu is not accounted for by TEM analysis. This "missing" Cu is believed to be in metallic clusters smaller than  $2$  nm in diameter. These smaller clusters are expected to absorb in the blue-green region of the optical spectra.

The volume fraction of the metal in clusters has a direct influence on the optical properties of these composite materials. Ion dose, dose rate and substrate temperature during implantation all affect the volume fraction of Cu found from TEM analysis. The volume fraction  $p$  is important for the both the linear absorption and the nonlinear response.

### Linear Optical Characterization

The measured optical absorption of the implanted glasses arises from the defects caused by the implantation process; from the implanted ion; and from interactions of both defects and implanted species with the substrate.

Ion implantation introduces the  $B_2$ ,  $E'$  peroxy and homobond defect centers in silica which exhibit absorption bands at 5, 5.8, 7.5 and 7.6 eV respectively.<sup>1</sup> However the production of defects as a function of implanted ion is dose dependent. This is established by the difference observed in EC for the different doses in the absorption regions assigned to the defect centers and from IR measurements. We suggest that with increasing cluster size and volume fraction of resolvable colloids that a greater disruption of the network occurs creating more broken bonds. This increase in broken and strained bonds gives rise to increased defect concentrations for higher dose and higher substrate temperatures. This interpretation is supported by infrared reflectance measurements.

The other source of absorption is the Cu clusters themselves. The optical properties of small metallic clusters were first studied by Mie.<sup>2,3,4</sup> For particles with diameters less than  $\lambda/20$  in diameter only the electric dipole interaction contributes to the absorption significantly which can be expressed as

$$\alpha = \frac{18\pi p n_d^3}{\lambda} \frac{e_2}{(e_1 + 2n_d^2)^2 + e_2^2} \quad (1)$$

where  $\alpha$  is the absorption,  $\epsilon(\lambda) = \epsilon_1 + i\epsilon_2$  is the dielectric constant of the metal,  $p$  is the volume fraction of the metal particles and  $n_d$  is the index of refraction of the dielectric. The absorption will have a maximum at the surface plasmon resonance where  $\epsilon_1 + 2n_d^2 = 0$ .

For metals the real part of the dielectric constant can be negative and is frequency dependent. Consequently the surface plasmon resonance frequency depends on the properties of the metal clusters. The simple Mie theory depends on cluster size through its effects on the dielectric constant of the metal particles.<sup>2,3,4</sup> The effects of smaller particle size is to increase the width, lower the absorption of the peak and shift the peak to longer wavelength. This difference in dielectric properties depending on size and on metal ion species opens the possibility for tailoring the optical properties of these metallic nanocluster composites.

More sophisticated theories of the optical properties of small particles predict different shifts of the absorption due to the induced dipole in the metal cluster depending on the dominant electronic mechanism contributing to the dielectric constant. A summary of size effects on the peak position predicted by different theories is given by Kreibig and Genzel.<sup>4</sup> Only very small shifts are expected ~2-5% for either blue shifts or red shifts. The most important affect on peak position appears to come from the contribution of bound electrons to the dielectric properties of the metal nanometer clusters which will vary with metal ion.<sup>2,4</sup> The width of the plasmon resonance peak increases with decreasing particle size while at the same time the magnitude of the absorption decreases. In addition to the optical characteristics of the colloids themselves, the plasmon resonance behavior and other linear and nonlinear optical characteristics of composite materials such as those we have produced will depend to a critical degree on the possibility of cluster-cluster interactions, lattice defects, shape factors, and surface roughness.<sup>2,4,5,6</sup>



Figure 4. Extinction coefficient as a function of energy for samples implanted with Cu dose of  $6 \times 10^{16}$  ions/cm<sup>2</sup>.

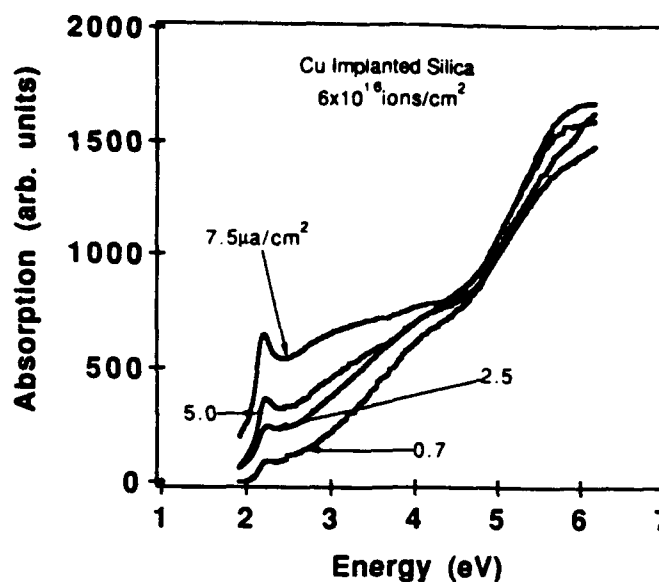
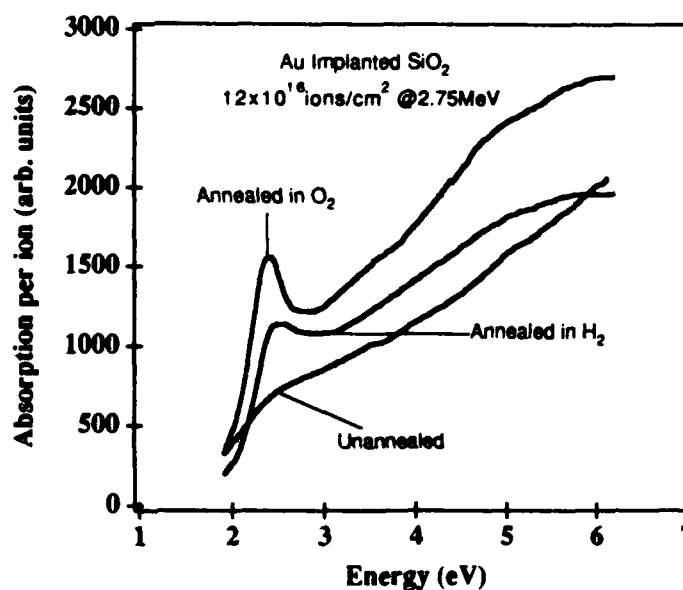


Figure 4 shows the optical absorption for a series of samples as a function dose rate for Cu implanted silica. The peak at 2.25 eV we attribute to the surface plasmon resonance of the Cu clusters. As predicted the absorption associated with the peak increases with increasing mean particle size and volume fraction of Cu detected by TEM as seen in the figure for four samples implanted with the same total dose but at different dose rates.

The absorption between 2.5–5 eV we attribute to the absorption of the metal clusters. The increased absorption with dose is due to two factors. As the dose increases so does both the mean particle size and the statistical distribution. At the highest dose some of the particles formed are sufficiently large that scattering and additional terms in Mie's expression are needed to fully describe the extinction. The extinction for scattering is proportional to  $1/\lambda^4$  and for absorption the extinction is proportional to  $1/\lambda$ . The second factor is the increase in volume fraction,  $p$ , of the metal in clusters. The absorption is expected to increase linearly with increasing volume fraction.

Figure 5. Extinction coefficient as a function of energy for samples implanted with Au dose of  $12 \times 10^{16}$  ions/cm<sup>2</sup>.



Shown in figure 5 is the optical absorption for the Au implanted silica for the sample implanted with a dose of  $12 \times 10^{16}$  ions/cm<sup>2</sup> for the as implanted sample, for the sample annealed in Ar+4% H<sub>2</sub> and for the sample annealed in O<sub>2</sub>.

We attribute the inflection at 2.4 eV in the as implanted sample and the peak in the annealed samples at 2.4 eV to the surface plasmon resonance of small Au nanoclusters. We estimate based on prior reports for gold colloids in water and glass that the size of the clusters to be <3nm in size for the as implanted sample with the mean size increasing with annealing. The increase in size with annealing is consistent with the optical absorption reported earlier for Au colloids in water ranging from 5–30 nm in diameter. The sharpening and increase in magnitude of this peak is also consistent with Mie theory for particles of this size. We attribute the linear increase in absorption in the other areas of spectra to the absorption dependence on  $1/\lambda$  as seen in equation 1. We speculate that the overall increase in absorption with annealing is due to an increasing volume fraction of Au colloids contributing to the surface plasmon resonance at 2.4 eV.

### Nonlinear Optical Characterization

Effective medium theory predicts that the effective third-order nonlinear susceptibility of the composite nanocluster material is dominated by the nonlinear optical response of the metal electrons.<sup>5,7,8</sup> The nonlinear susceptibility  $\chi_{eff}^{(3)}$  of the composite is related to the  $\chi_m^{(3)}$  of the metal clusters by the following

$$\chi_{eff}^{(3)} = p \left( \frac{3n_d}{\epsilon + 2n_d^2} \right)^4 \chi_m^{(3)} \quad (2)$$

where  $p$  is the volume fraction of the metal clusters,  $\epsilon$  is the total complex dielectric function of the metal,  $n_d$  is the dielectric function of the dielectric host and  $\chi_m$  is the third order susceptibility of the metal colloids. Thus, increasing the volume fraction increases the linear absorption as well as the effective third order susceptibility.

The nonlinear index of refraction  $n_2$  is defined in terms of the ordinary linear index  $n_0$  and the complex third order nonlinear dielectric susceptibility  $\chi^{(3)}$  by the following equations

$$n = n_0 + n_2 I \text{ and } n_2 = \frac{4\pi}{3n_0} 10^{-8} \text{Re}[\chi^{(3)}] \quad (3)$$

where  $n_0$  is the linear index of refraction and  $I$  is the laser intensity. The local field enhancement factor given by the term in parenthesis in equation 2 will be large on or in the vicinity of plasmon resonance frequency given by  $\epsilon + 2n_d^2 = 0$ . We measured the nonlinear index of refraction using a variation of the so-called Z-scan technique.<sup>9</sup> We observe this increase in  $n_2$  as we approach the plasmon resonance in the Cu implanted silica as seen in figure 6 for a sample implanted to a dose of  $12 \times 10^{16}$  ions/cm<sup>2</sup>.

Figure 6. Measured values of  $\chi^{(3)}$  for sample with dose of  $12 \times 10^{16}$  ions/cm<sup>2</sup>, superimposed on a section of the absorption spectra.

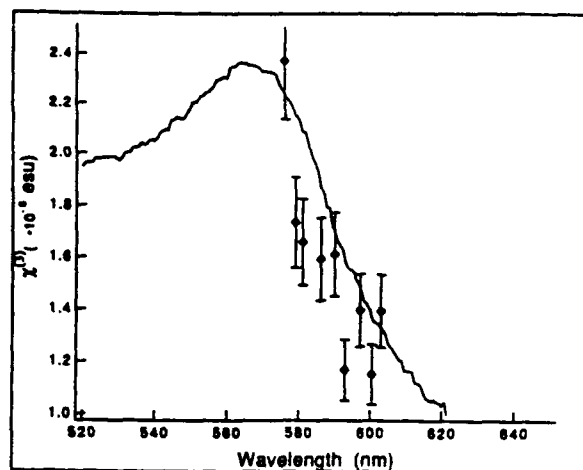


Table 4  
Z-scan results for circular polarized light @ 575nm with laser pulse width of 5ps  
for Cu implanted silica with nominal dose of  $6 \times 10^{16}$  ions/cm<sup>2</sup>

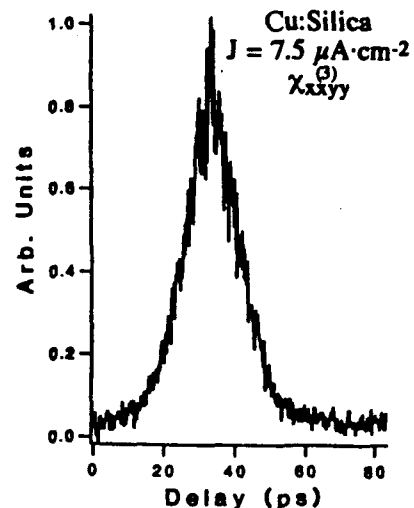
Dose Rate	$n_2 (\times 10^{-9} \text{cm}^2/\text{W})$	Mean Particle Size (nm)	Vol. Fraction (%)
$7.5 \mu\text{A}/\text{cm}^2$	1.3	12.6	4.8
$5.0 \mu\text{A}/\text{cm}^2$	1.0	9.9	2.8
$2.5 \mu\text{A}/\text{cm}^2$	0.8	6.7	1.8
$0.7 \mu\text{A}/\text{cm}^2$	0.4	5.2	0.9

Table 4 gives the Z-scan results for the samples implanted with  $6 \times 10^{16}$  ions/cm<sup>2</sup> at a series of dose rates at a wavelength of 575nm. The values for  $n_2$  increase with increasing dose rate. The total amount of Cu is the same in each sample. However the volume fraction of the Cu in colloids detectable with TEM increases with increasing dose rate as shown in Table 4. Also shown in Table 4 is the mean particle size. The increase in  $n_2$  scales with both variables. We would expect from measurements on gold colloids in water (5–30nm in diameter)<sup>5,7</sup> that the particle size would not exhibit a large effect on  $n_2$  and based on the mechanism responsible for  $\chi^{(3)}$  we do not expect a significant size dependence.<sup>5,7</sup> As a result we attribute at present the increase in  $n_2$  to the increase in volume fraction of the Cu detected in colloids >2nm. This increase with volume fraction is in accordance also with equation 2 where the increase in effective  $\chi^{(3)}$  increases with volume fraction.

The Z-scan measurements cannot give a direct measurement of the temporal response of the metal clusters. In order to ascertain the time scale of the nonlinear optical response, we carried out a limited series of forward degenerate four-wave mixing (DFWM) measurements on some of our samples. These measurements were carried out in the Ultrafast Spectroscopy Laboratory at the City University of New York using facilities generously placed at our disposal by Prof. Robert Alfano of CUNY. The forward DFWM measurements were made using a mode-locked Q-switched, frequency doubled Nd: YAG laser operating at a wavelength of 532 nm at a pulse repetition frequency of 10 Hz, with a pulse duration of 35 ps. This wavelength is well off the plasmon resonance for Cu, but close to the plasmon resonance for the Au implanted silica. Figure 7 shows the phase conjugate signal as a function of pump probe delay time from the

DFWM measurement on a sample implanted with Cu to a dose of  $6 \times 10^{16}$  ions/cm<sup>2</sup>. From these experiments we determine that the response is no slower than 15 ps. Based on the low pulse repetition rate of the laser and the speed of the response, we attribute the ultrafast nonlinear response to an electronic Kerr type nonlinearity for both the Au and Cu implanted silicas.

Figure 7. Phase conjugate signal from DFWM measurement for  $\chi^{(3)}$  component from samples implanted with Cu dose of  $6 \times 10^{16}$  ions/cm<sup>2</sup>.



There is essentially no change in the  $\chi^{(3)}$  values for the as implanted sample and the annealed samples for silica implanted with Au to a dose of  $6 \times 10^{16}$  ions/cm<sup>2</sup>. There is an increase in  $\chi^{(3)}$  between the as-implanted and annealed samples for silica implanted with  $12 \times 10^{16}$  Au ions/cm<sup>2</sup>. The lack of particle size effect for magnitude of the response has been observed by Bloemer et al.<sup>5</sup> for Au particles in water. We attribute the difference in  $\chi^{(3)}$  for the different doses to a difference in the volume fraction of Au present in accordance with equation 2. The Cu implanted silica samples show similar behavior for the DFWM experiments.

Hache et al.<sup>7</sup> have identified three mechanisms that contribute to the nonlinear response in varying proportions depending on the detailed electronic structure of the metal cluster and the laser wavelength. These mechanisms are: (1) Intraband transitions. The contribution to  $\chi^{(3)}$  from this mechanism is predicted to vary as  $1/r^3$ . For gold the  $\chi^{(3)}$  contribution for this mechanism is predicted to be  $\sim 10^{-10}$  esu at 532 nm. (2) Interband transitions. Absorptive optical transitions from the localized d-bands to the s-p conduction band should depend on details of the electronic structure of the metal cluster, but be both size and shape independent. The contribution to  $\chi^{(3)}$  from this mechanism is mostly imaginary; for gold at 532 nm, it has a magnitude  $\sim 1.7 \times 10^{-4}$  esu. (3) Hot-electron transitions. Nonequilibrium heating of the electrons in the conduction band leads to Fermi-level smearing which changes the electron occupancy near the Fermi level. By changing the electron energy distribution, this contribution also changes the macroscopic dielectric function of the electron gas.

Hache et al.<sup>7</sup> show that the hot electron contribution to  $\delta\epsilon_m$  is given by

$$\delta\epsilon_m = \frac{24\pi^2}{nc} \chi_m^{(3)} f^2 I_0 \quad (4)$$

where  $I_0$  is the incident intensity,  $n$  is the index of the composite material and  $f$  is the local field factor given by  $3n_d/(\epsilon + 2n_d^2)$ , the same local field factor seen in equation 2. This mechanism has no size dependence, and is calculated for gold spheres to dominate the intraband transition probability by two orders of magnitude for 5nm particles at wavelengths near the surface plasmon resonance. The hot-electron contribution to  $\chi^{(3)}$  is mostly imaginary and is predicted to be  $\sim$

$1.1 \times 10^{-7}$  esu for gold colloids. A response time of 2–3 ps is predicted for this mechanism based on the time for the electrons to equilibrate with the lattice.

### Summary of Results for Au Implanted $\text{Al}_2\text{O}_3$

Limited implantation of Au into single crystal  $\text{Al}_2\text{O}_3$  was made because of the importance of  $\text{Al}_2\text{O}_3$  for devices. The samples were gold in color but with annealing turn deep purple. After annealing the colloids were found from TEM analysis to be on the average  $\sim 8$  nm in size. The colloids ranged from 2 to 60 nm in size. Figure 8 shows the optical absorption for a series of Au implanted  $\text{Al}_2\text{O}_3$ . Preliminary DFWM experiments suggest that the nonlinear response was similar to that for the Au implanted silica. The mechanism is thought to be the same as that for the Au implanted silica.

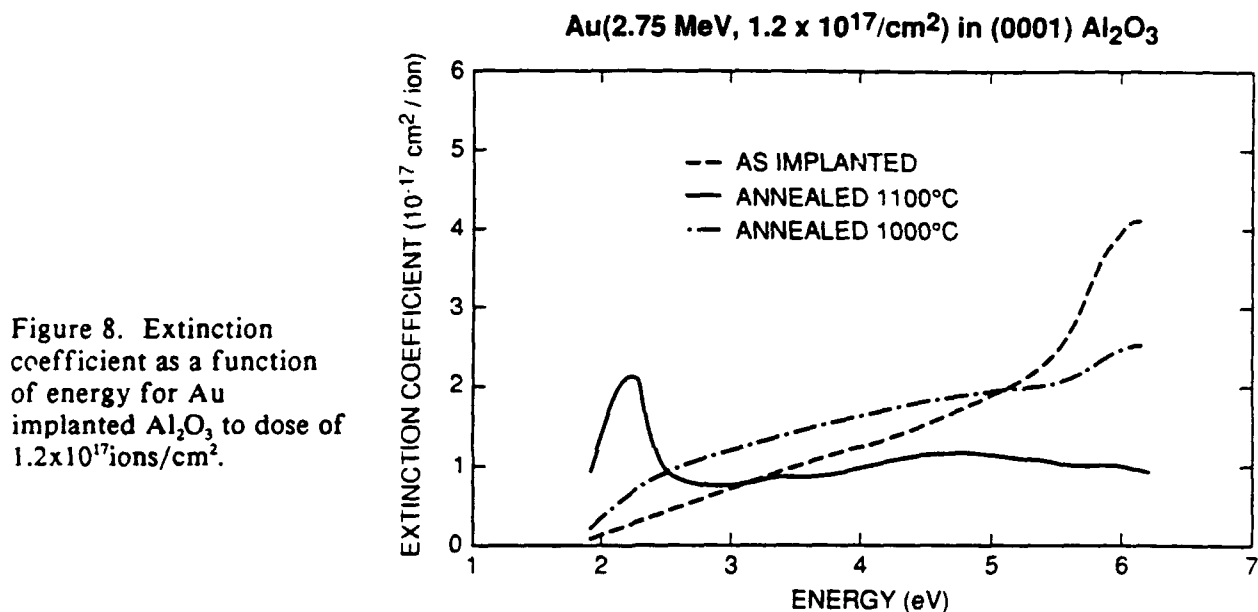


Figure 8. Extinction coefficient as a function of energy for Au implanted  $\text{Al}_2\text{O}_3$  to dose of  $1.2 \times 10^{17}$  ions/cm<sup>2</sup>.

### Implications for Bistable Device Development

The development of practical optical computing and communication devices will require optically bistable materials which can be fabricated by techniques compatible with microelectronics processing technology. Optical requirements for photonic devices require not only a large  $\chi^{(3)}$  and short switching length  $L_{\pi}$  for a phase shift of  $\pi$ , but also  $(\alpha + \beta I) \cdot L_{\pi} \leq 0.1$ , where  $\alpha$  and  $\beta$  are the total (absorption + scattering) and two-photon absorption coefficients, and  $I$  is the laser intensity. Device reliability further demands long-term material stability under high-intensity laser irradiation, and practical device sizes will dictate that  $L_{\pi}$  be of micron dimensions.

It is well known that low two-photon absorption is one of the most important characteristics required of practical bistable devices. We have made no direct measurements of the two-photon absorption, but detailed fitting of the Z-scan spectra requires that one include the two-photon absorption coefficient  $\beta$ . Analysis of Z-scan spectra for both 5.5 ps and 100 ps pulses indicates that the two-photon absorption is not a large effect for our experiments; we estimate  $0.1 \leq \beta \leq 1 \text{ cm} \cdot \text{GW}^{-1}$ .

The device potential for a given material clearly depends not only on the ease of fabrication but also on the device parameters. In the present case, we calculate that the switching

length in a waveguide made by ion implantation in silica is  $L = \sim 3-5 \mu\text{m}$ . Hence the nonlinear figure-of-merit<sup>10</sup>

$$0.2 \leq F = 2\lambda \frac{\beta}{\gamma} \leq 2.0 \quad (5)$$

In general, one would like to have a figure of merit less than 1. The figure-of-merit for our nanocluster composite materials is clearly in the interesting range. Moreover, there are many reasons to believe that optimized composite materials have yet to be produced by this technique.

By controlling nanocluster properties, it may be possible to tailor the optical properties of these composites for specific applications in optical waveguides and other devices, as well as to enhance the nonlinear optical response through appropriate choice of the host matrix. The inherent flexibility of the ion implantation process is particularly intriguing in light of predictions<sup>11,12</sup> of large enhancements in the third-order nonlinearity for metal-dielectric composite structures created in a nonlinear host matrix.

### Personnel

Since March 1, 1991, research on optical bistability in metallic copper clusters created by ion implantation has been supported at Vanderbilt University by the Army Research Office through contract DAAL03-91G-0028 for a one-year exploratory research project. Prof. Robert H. Magruder, III, the principal investigator, was supported during this period. Prof. Richard Haglund was a faculty collaborator during this period. One Ph.D. student, Ms. Li Yang, has been supported by the grant during this period; Ms. Yang expects to complete the work for the Ph.D. degree in late 1992.

### References

1. G.W. Arnold, "Ion Implantation Effects in Glasses," *Rad. Eff.* **65** (1982) 17-30; A.R. Bayly, "Optical Properties of Ion Bombarded Silica Glass," *Rad Eff.* **18** (1973) 111-118; M. Antonini, P. Camagni, P.N. Gibson and A. Manara, "Comparison of Heavy Ion, Proton and Electron Irradiation Effects in Vitreous Silica," *Rad. Eff.* **65** (1982) 41-48.
2. C.F. Bohren and D.R. Huffman, *Absorption and Scattering of Light by Small Particles*, John Wiley and Sons, New York, 1983.
3. G.W. Arnold and J.A. Borders, "Aggregation and Migration of Ion-Implanted Silver in Lithia-Alumina-Silica Glass," *J. Appl. Phys.* **48** (1977) 1488-1496.
4. U. Kreibig and L. Genzel, "Optical Absorption of Small Metallic Particles," *Sur. Sci.* **156** (1985) 678-700.
5. M.J. Bloemer, J.W. Haus and P.R. Ashley, "Degenerate Four Wave Mixing in Colloidal Gold as Function of Particle Size," *J. Opt. Soc. Am.* **B7** (1990) 790-795.
6. U. Kreibig, "Lattice Defects in Small Metal Particles and Their Influence on Size Effects," *Z. Physik B31* (1978) 39-47.
7. F. Hache, D. Ricard and C. Flytzanis, "Optical Nonlinearities of Small Metal Particles: Surface Mediated Resonance and Quantum Size Effects," *J. Opt. Soc. Am.* **B3** (1986) 1647-1655.

8. D. Ricard, P. Roussignol and C. Flytzanis, "Surface Mediated Enhancement of Optical Phase Conjugation in Metal Colloids," *Opt. Letts.* 10 (1985) 511-513.
9. M. Sheik-Bahae, A.A. Said, T. Wei, D.S. Hagan and E.W. Van Stryland, "Sensitive Measurement of Optical Nonlinearities Using a Single Beam," *IEEE J. Quantum Electronics*, 26 (1990) 760-769.
10. V. Mizrahi, K.W. DeLong, G.I. Stegeman, M.A. Saifi and M.J. Andrejco, "Two Photon Absorption as a Limitation to All Optical Switching," *Opt. Lett.*, 14 (1989) 1140-1142.
11. J.W. Haus, N. Kalyaniwalla, R. Inguva, M. Bloemer and C.M. Bowden, "Nonlinear-Optical Properties of Conductive Spheroidal Particle Composites," *J. Opt. Soc. Am. B6* (1989) 797-807.
12. A.E. Neeves and M.H. Birnboim, "Composite Structures for the Enhancement of Nonlinear Optical Susceptibility," *J. Opt. Soc. Am. B6* (1989) 787-796, and E.A. Neeves and M.H. Birnboim, "Composite Structures for the Enhancements of Nonlinear Optical Materials," *Opt. Lett.* 13 (1988) 1087-1089.

## Publications

The following papers and presentations acknowledging support of the Army Research Office has been published or are in preparation:

1. "Nonlinear Index of Refraction of Cu- and Pb-Implanted Fused Silica," R.F. Haglund, Jr., R.H. Magruder, III, S.H. Morgan, D.O. Henderson, R.A. Weller, L. Yang and R.A. Zuhr, Nuclear Instruments and Methods in Physics Research B65 (1992) 405-421.
2. "Nonlinear Optical Behavior of Cu Nanocluster Layers Created by Ion Implantation," R.F. Haglund, Jr., R.H. Magruder, III, L. Yang, J.E. Wittig and R.A. Zuhr, to be published in proceedings of the International Conference on the Physics and Chemistry of Finite Systems, a volume in the NATO proceedings series (Kluwer Academic Publishers, 1992).
3. "Picosecond Nonlinear Optical Response of Copper Clusters Created by Ion Implantation in Fused Silica," R.H. Magruder, III, R.F. Haglund, Jr., L. Yang, J.E. Wittig, K. Becker and R.A. Zuhr, in "Optical Waveguide Materials," Proc. Mat. Res. Society 244 (1992), 369-374.
4. "Picosecond Third-Order Susceptibility of Cu-Ion-Implanted Fused Silica," R.F. Haglund, Jr., L. Yang, K. Becker, R.H. Magruder, III, J.E. Wittig and R.A. Zuhr, submitted to Opt. Lett.
5. "Optical and Infrared Spectroscopy of Laser Irradiated Bi-Implanted Silica," R.H. Magruder, III, D.O. Henderson, S.H. Morgan and R.A. Zuhr, in Ion-Beam Modification of Materials, Proc. Mat. Res. Society 235 (1992), 383-388.
6. "Nonlinear Index of Refraction Measurements in Submicron Layers," L. Yang, K. Becker and R.F. Haglund, Jr., to be submitted to Opt. Lett.
7. "Effects of Ion Dose Rate on the Size Distribution and Nonlinear Optical Properties of Cu Clusters Created by Ion Implantation," R.H. Magruder, III, J.E. Wittig, R.A. Zuhr, L. Yang and R.F. Haglund, Jr., to be submitted to J. Appl. Phys. (in preparation).
8. "Modification of the Optical Properties of  $Al_2O_3$  by Ion Implantation," C.W. White, D.K. Thomas, R.A. Zuhr, J.C. McCallum, A. Pogany, R.F. Haglund, R.H. Magruder, III, and L. Yang, MRS Proceedings, Symposium A, Spring Meeting 1992, in press.
9. "Structure Property Relationships of Nanometer Size Metal Clusters in Glasses," R.H. Magruder, III, D.L. Kinser, J.E. Wittig and R.A. Zuhr, in press, SPIE Properties and Characteristics of Optical Glass III, San Diego, July 1992.
10. "Colloidal Au Precipitates Formed by Ion Implantation and Thermal Annealing," C.W. White, D.K. Thomas, D.K. Hensely, R.A. Zuhr, J.C. McCallum, A. Pogany, R.F. Haglund, R.H. Magruder, III, and L. Yang, submitted to First International Conference on Nanostructure Materials, Cancun, Mexico, September 1992.
11. "Picosecond  $\chi^{(3)}$  of Metal-Nanocluster-Glass Composites Made by Ion Implantation," R.F. Haglund, L. Yang, R.H. Magruder, III, R.A. Zuhr and C.W. White, submitted to Conference on Nonlinear Optical Properties of Advanced Materials OE/LASER '93.



12. "Optical Properties of Gold Nanoclusters Formed by Ion Implantation in Silica," R.H. Magruder, III, R.F. Haglund, L. Yang and C.W. White, to be submitted to Applied Physics Letters (in preparation).
13. "A Vibrational Analysis of Au Implanted  $\text{Al}_2\text{O}_3$  Single Crystals: Ion and Thermal Annealing Affects," submitted to MRS Fall Meeting, Boston, 1992, Beam Solid Interactions, proceedings to be published.

Support from the ARO is also acknowledged in the following conference presentations:

1. "Theory of Nonlinear Index of Refraction Measurements in Thin Layers," L. Yang, K. Becker and R.F. Haglund, Jr., Bull. Am. Phys. Soc. (1991).
2. "Picosecond Optical Nonlinearity of Cu Nanoclusters Made by Ion Implantation," R.F. Haglund, Jr., L. Yang, K. Becker, R.H. Magruder, III, J.E. Wittig and R.A. Zuhr, submitted to International Conference on Quantum Electronics, June 1992.
3. "Optical Properties of Small Metal Clusters Formed in Silica by Ion Implantation," R.H. Magruder, III, Gordon Conference on Optical Phenomena in Glass, Tilton, NH, June 29, 1992.
4. "Picosecond Optical Bistability in Metal Nanocluster Composites," R.F. Haglund, Gordon Conference on Particle-Solid Interactions, Plymouth, NH, July 8, 1992.
5. "Polarization and Size Dependence of Third Order Nonlinearities of Metallic Quantum Dots Embeddeed in Glass Matrix," L. Yang, K. Becker, S.W. Brown and R.F. Haglund, Optical Society of America annual conference, Albuquerque, New Mexico, September 20, 1992.